Wind and Structures, *Vol. 30, No. 2 (2020) 211-217*
DOI: https://doi.org/10.12989/was.2020.30.2.211

Dynamic behavior of smart material embedded wind turbine blade under actuated condition

Yuvaraja Mani, Jagadeesh Veeraragu*, Sangameshwar S. and Rudramoorthy Rangaswamy

Department of Mechanical Engineering, PSG college of Technology, Peelamedu, Coimbatore, Tamilnadu-641004, India

(Received September 10, 2018, Revised June 1, 2019, Accepted November 26, 2019)

Abstract. Vibrations of a wind turbine blade have a negative impact on its performance and result in failure of the blade, therefore an approach to effectively control vibration in turbine blades are sought by wind industry. The small domestic horizontal axis wind turbine blades induce flap wise (out-of-plane) vibration, due to varying wind speeds. These flap wise vibrations are transferred to the structure, which even causes catastrophic failure of the system. Shape memory alloys which possess physical property of variable stiffness across different phases are embedded into the composite blades for active vibration control. Previously Shape memory alloys have been used as actuators to change their angles and orientations in fighter jet blades but not used for active vibration control for wind turbine blades. In this work a GFRP blade embedded with Shape Memory Alloy (SMA) and tested for its vibrational and material damping characteristics, under martensitic and austenite conditions. The embedment portrays 47% reduction in displacement of blade, with respect to the conventional blade. An analytical model for the actuated smart blade is also proposed, which validates the harmonic response of the smart blade.

Keywords: wind turbine blade; smart blade; Ni-Ti alloy; actuation; Shape Memory Alloy (SMA)

1. Introduction

Vibrational problems in the domestic horizontal axis wind turbines are due to flap wise and edge wise vibrations among which the flap wise vibrations are the most predominant due to the varying wind velocities acting perpendicular to its surface (Kumar *et al.* 2014). It has been reported that monitoring the structural health of the turbine blades requires special attention as they are key elements of a wind power generation, and account for 15-20% of the total turbine cost. Recent studies also indicate that blade damage as the most expensive type of damage to repair and can cause serious secondary damage to the wind turbine system due to flap wise vibrations Pabut *et al.* (2012).

The natural frequencies are critical component of a given structure (Cromack 1978), which when matched by external forcing frequency induces resonance of the structure. The resonance of the structure, leads to failure of the said structure or transmits awkward vibrations to coupled system. Thus the structure must be designed in such a way to avoid the occurrence of resonance and if the resonance cannot be avoided, then it should facilitate damping, thus reducing the vibration intensity. As the wind turbine blades are subjected to varying wind velocities, a vibration control method has to be provided, which adapts to the vibration of the structure. Thus keeping vibration of blade to a limited level. In this article, a blade with shape memory alloy actuator wire has been developed and its vibration characteristics are compared to the conventional blade.

*Corresponding author, Ph.D. Student
E-mail: Jagan047@gmail.com

For SMA wires, the inelastic strain induced a result of phase transformation of material from martensite to austenite. With the internal resistance of SMA wires being high, supply of electric current causes the wires to induce heat. The SMA undergoes up to 8% strain upon heating and returns to its original length upon cooling, due to its shape memory effect (Bhargaw *et al*. 2013). The merits of SMA in shape memory applications are studied in detail by Umesh and Ganguli (2009), Hu and Vukovich (2005), Vitiello *et al*. (2005), Seelecke and Müller (2004) has explored the use of SMA actuators in smart materials. Static and dynamic shape control of structures by piezoelectric actuation is reviewed by Irschik (2002). Choi and Lee (1998) has investigated the shape control of composites beam with SMA wires. The performance of SMA actuator for prosthetic hand are well explored by O'Toole *et al*. (2009). Recent research in smart materials shows their potential for changing the configuration of airplane wing to improve aerodynamic performance and shows that they can eliminate the complexity and bulkiness of the actuating systems that are used in conventional wings Kim and Cho (2010). The general idea of changing the wing configuration for this concept is to induce strain in the structure by interfacing with smart materials. In this paper, small horizontal axis wind turbine blade will be manufactured with SMA wires and the vibration characteristics of SMA embedded blade will be compared with the conventional wind turbine blade.

SMA possesses shape-memory property, which the metal recovers to its original size or shape and reverts to it at a characteristic transformation temperature. These alloys change phase (between martensitic and austenite) at certain critical temperatures and therefore SMA displays different stress-strain characteristics at different temperature ranges. The thermo-electric behavior of Ni-Ti shape memory alloy

http://www.techno-press.com/journals/was&subpage=7 ISSN: 1226-6116 (Print), 1598-6225 (Online)

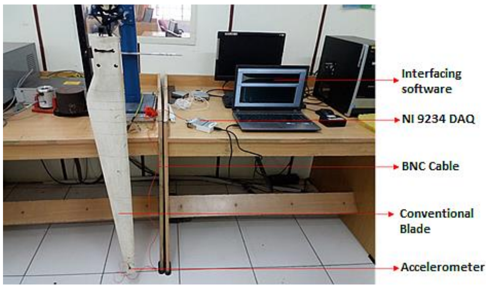

Fig. 1 Experimental modal analysis

Fig. 2 Experimental harmonic excitation of conventional blade

wires has been analyzed by (Bhargaw *et al.* 2013). These characteristics of SMA is used for analytical model for the smart blade, under actuated conditions.

2. Vibration characteristics of conventional wind turbine blade

Conventional domestic wind turbine blade with NACA 4418 profile, with 1kW power production capability is evaluated for its vibration characteristics. The vibration characteristics of the blade, namely natural frequency and damping, are evaluated through modal analysis as Sellami *et al.* (2016). The actual amplitude of vibration at resonance is evaluated using harmonic analysis.

2.1 Experimental modal analysis on conventional blade

The glass fiber based conventional blade is evaluated for the dynamic properties by performing the experimental modal analysis using an impact hammer. The experimental setup is shown in Fig. 1.

The blade is excited with an impulse force using the impact hammer and the time based acceleration readings are collected through an interfacing software. The time domain signal is converted to frequency domain signal by performing Fast Fourier Transform (FFT). The frequency domain signal depicts that the natural frequency of the blade is 26 Hz. The time based response is evaluated for damping of the blade, using logarithmic decrement method Mevada and Patel 2016. The damping of the conventional blade is calculated to be 0.0103.

2.2 Experimental harmonic analysis on conventional blade

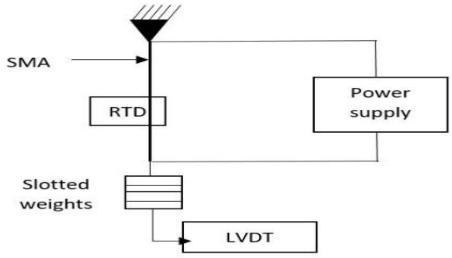

Fig. 3 Block diagram of characteristic study

Chen *et al.* (2016) evaluated wind load as combination of harmonic loading and Martinez-Vazquez (2016) studied the influence of wind induced structural vibrations around the resonant frequency of the structure. Hence, the influence of resonance can be studied using harmonic analysis and reduction in resonance amplitude, corresponds to the improved integrity of the blade. The blade is mounted on the electro dynamic shaker and an accelerometer is used to export the time domain signals. The experimental setup used for evaluation is shown in Fig. 2.

The response of the blade is collected using an interfacing software. Mollasalehi *et al.* 2013 categorized first bending mode of wind turbine blade is prominent to induce noise and vibration. Hence the harmonic analysis on the blade is performed with 9.81 ms-2 of input acceleration and excitation frequency range of 20 Hz to 40 Hz which shows the respective maximum deflection 11.4 mm achieved for corresponding natural frequency of the blade, 25 Hz.

3. Shape Memory Alloy (SMA) in vibration control

SMA has shown a huge potential in vibration control, through its super elastic and shape memory effect. Though various studies, such as Ni *et al.* (2007), Lau (2002) have been made with SMA on composites, limited characteristic study has been made on SMA embedded wind turbine blade. Evaluation of SMA characteristics is primary to study the influence of SMA on wind turbine blade.

3.1 Characterization of SMA properties

The characterization of 0.5 mm diameter Nitinol wire of length 180 mm is evaluated under pre stressed condition under martensitic and austenite conditions. The SMA wire is coupled to slot weights in order to induce stress. The characterization of SMA is performed by following the procedure of Bhargaw, Ahmed, and Sinha (2013). The block diagram of the experimentation is shown in Fig. 3.

The experimentation is limited to the austenite transition temperature of 90^{o}C, within which the actuation is to be provided to SMA embedded blade. The potential of SMA to offer high electrical resistance is utilized to heat the SMA and induce the phase transformation. The SMA is pre-stressed to various levels such as 12.49 MPa, 27.47 MPa and 37.47 MPa, by loading the wire under 0.25 kg, 0.5 kg and 0.75 kg.

A Resistance Temperature Detector (RTD) is connected

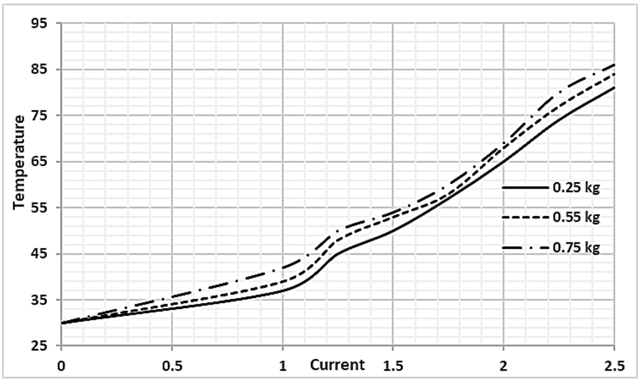

Fig. 4 Current Vs Temperature

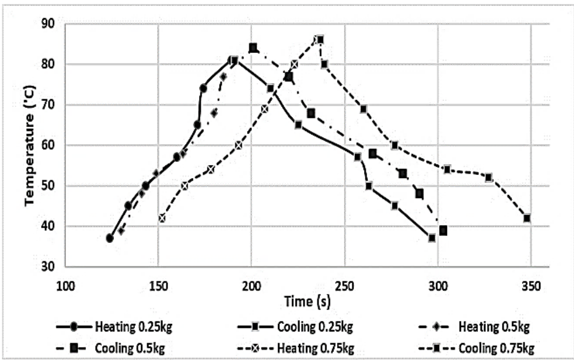

Fig. 5 Variation of Heating and cooling time with different load

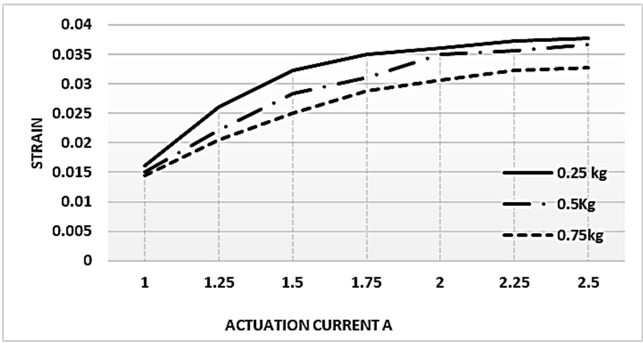

Fig. 6 Strain produced across actuation current

across the wire and its temperature increase across different heating conditions are studied. The current is provided across the SMA wire at increments of 0.5A and the temperature induced is noted. Fig. 4 shows the increase of temperature across the flow of electricity.

The time taken for the SMA to heat and cool to the corresponding actuation current is depicted in the figure 5. The phase transformation of SMA also induces reduction in length of SMA, the Linear Variable Differential Transformer (LVDT) connected across the SMA depicts the amount of strain in the length of SMA.

The strain produced across the SMA, at different actuation current and applied stress is plotted in the figure 6. The strain induced in SMA on actuation is used for deducting the empirical relation between actuation current

The displacement thus induced in the SMA can be visualized in Fig. 7, which depicts the hysteresis cycle

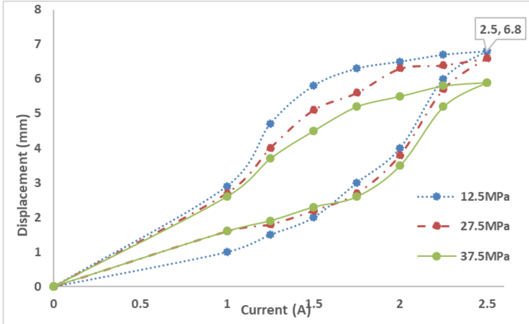

Fig. 7 Displacement produced across actuation

Table 1 Variation of young's modulus with actuation

Actuation current (A)	0	1	1.5	2	2.5
Young's Modulus (GPA)	15.00	23.08	33.42	41.28	48.46

between heating and cooling of the SMA wire, under different actuations

The stress-strain variation can be used to derive the variation of young's modulus of SMA across the phase transformation. The tensile modulus of SMA at martensite condition is 15 GPa, the increase in the young's modulus of the SMA across actuation is portrayed in Table 1.

The change in young's modulus of SMA can be used to derive the analytical model for martensitic fraction. The empirical relation between martensitic fraction (ξ) and young's modulus of SMA, under actuation can be fitted using regression. The regression equation obtained for the young's modulus, across actuation is given as

$$E_S(\xi) = \ \alpha \ (\xi)^2 + \beta \ (\xi) + E_A \tag{1}$$

Where the coefficients of residuals α and β are -17.671 and 16.805 respectively. E_A is the young's modulus of SMA at austenite condition.

4. Vibration characteristics of smart wind turbine blade

With application of smart materials in structures by researchers such as Simonović *et al.* (2016), Lin *et al.* (1999), Lee *et al.* (2014), has experimentally showcased the vibration control using smart materials. Yet the influence of SMA on structures, under actuation has not been elaborated. In order to study the influence of SMA embedded wind turbine blade, a smart blade is developed, with 2 meter of 0.5 mm diameter SMA embedded inside. The volume fraction of SMA embedded inside the blade is 0.073% of volume of the composite wind turbine blade. The conventional and smart wind turbine blade are displayed in figure 8.

4.1 Modal analysis on smart blade

Similar to the modal analysis performed on conventional blade, the SMA embedded smart blade is evaluated for its

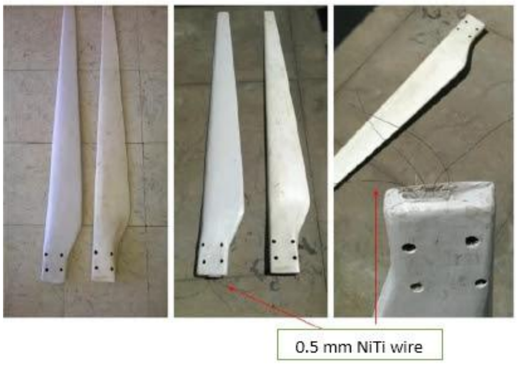

Fig. 8 Conventional and smart wind turbine blade

Table 2 Comparison of natural frequency

Mode	Convectional Blade (Hz)	Smart Blade (Hz) (Martensitic)	Smart Blade (Hz) (Austenite)		
			1.0 A	1.5 A	2.0 A
I	25	30	31	31	32
II	60	73	88	88	89

Table 3 Comparison of damping ratio

Convectional Blade	Smart Blade (Martensite)	Smart Blade (Austenite)		
		1.0 A	1.5 A	2.0 A
0.0103	0.0203	0.0330	0.0368	0.0422

vibrational characteristics at martensitic and austenite conditions of SMA. The martensitic condition corresponds to the experiment performed on the smart blade without actuation and the austenite condition refers to the actuation of SMA above its austenite start state.

The current is supplied from the variable power supply to the SMA wire and due to the resistance, the SMA wires tends to heat up. The rise in temperature, induces the shape memory effect of the wires, causing the SMA wire to contract causing the changes in the stiffness of the material (Song *et al*. 2000). The austenite start state of the SMA wire is 45^{o}C, which the material crosses by 1A. The natural frequency and damping ratio for different current supplied are studied.

Mollasalehi *et al*. (2013) has observed that the first bending mode plays a crucial role in generating vibration and noise. Hence, the first natural frequency of the blade is concentrated. The modal test has been carried out on the smart blade and a 16.67% shift in the first natural frequency for conventional wind turbine blade at martensitic phase is visualized. When current in supplied (1A,1.5A) to smart wind turbine blade there is a 3.22% shift from the first natural frequency of smart blade at martensitic phase. When 2A current is passed to smart blade a 6.25% of shift in the first natural frequency of smart blade at austenite was observed.

The damping ratio found for different actuating conditions and its comparison is tabulated in table 3.

There is a 49.26% increase in the damping ratio for smart wind turbine blade at martensitic phase. When current of 1A, 1.5A and 2A current is supplied its observed that there is 38.48%, 44.83% and 51.89% increase in the damping ratio at austenite phase respectively.

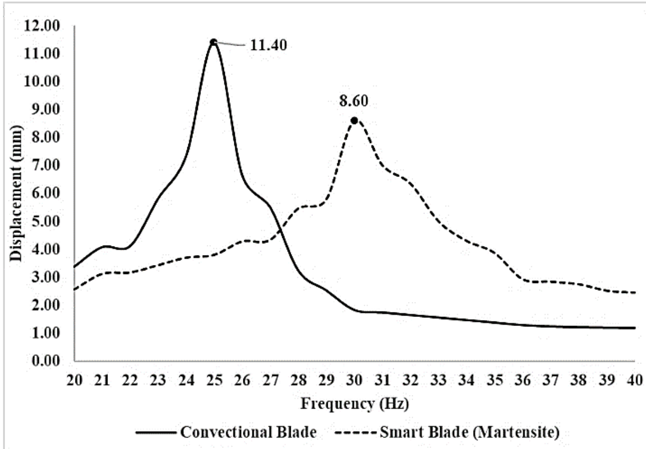

Fig. 9 Comparison of harmonic response for conventional and smart wind turbine blade(martensite)

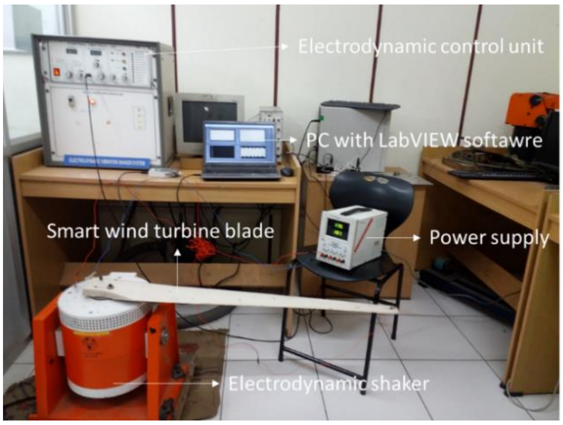

Fig. 10 Experimental harmonic response of smart blade with actuation

5. Experimental harmonic analysis

The impact of the increase in damping ratio of martensite and austenite conditions of smart blade can be validated by performing harmonic excitation on the smart blade. Mouleeswaran *et al.* (2018) performed harmonic analysis on small wind turbine blade to study the impact of resonance on the structure. Feng and Gomez-rivas (2005) evaluated the natural frequency of beam through frequency domain analysis, using piezo-electric accelerometer.

5.1 Harmonic response at martensitic phase

The harmonic response test has been carried out similarly on smart blade, using electro dynamic shaker. The smart blade is kept below the austenite start temperature (at room condition). The response of the smart blade under excitation frequency are acquired and plotted against the response of conventional blade. Fig. 6 denotes the response curve, plotted between displacement (mm) and frequency (Hz), comparing responses of conventional and smart blade. It depicts that the natural frequency of the smart blade, has shifted to 30Hz and resonating at 8.60 mm.

With embedment of SMA wires, the increase in the damping value of the smart blade is depicted in the decrease

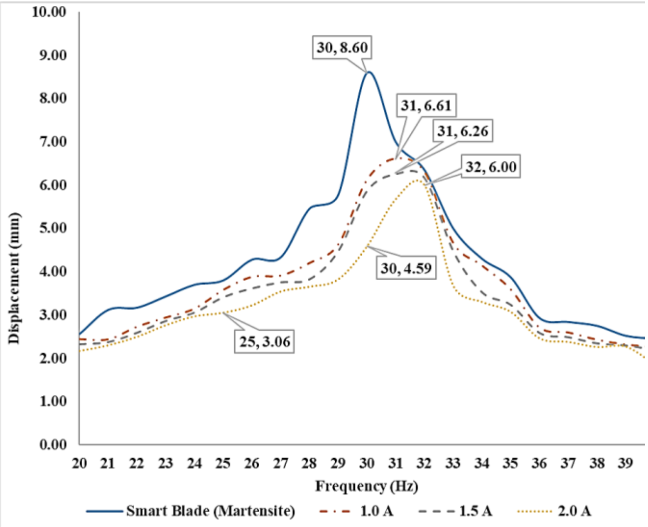

Fig. 11 Harmonic response of smart blade at Austenite phase

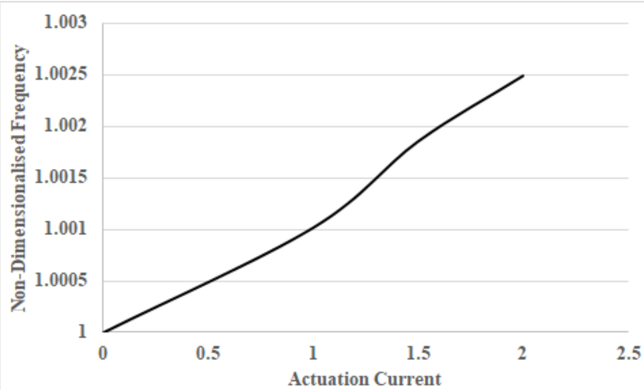

Fig. 12 Variation of Magnification factor across actuation current

of amplitude of vibration at resonance condition. The increase in young's modulus results in the increase of stiffness of blade. Thus increasing the natural frequency of the smart blade.

5.2 Harmonic response at austenite phase

In order to study the influence of actuation current of SMA on amplitude of vibration, actuation current of 1A to 2A is supplied in successions of 0.5A to the smart blade. As the smart blade is actuated, the resistance of SMA tend to heat up the wire. As the wire reaches austenite phase, the stiffness of the smart blade tends to increase. The smart blade is actuated at different actuation currents and their response along the natural frequency is evaluated. The experimental setup is shown in the Fig. 10.

The response of the smart blade, along the first natural frequency is shown in the Fig. 11. The response graph shows that there is 3.22% shift in first natural frequency when smart blade is excited with 1A and 1.5A but the reduction of displacement for 1A is 23.14% whereas there is 27.21% of decrease in the displacement at the 30 Hz.

When SMA wire is supplied with current of 2A there is

Table 4 Geometric and physical parameters of SMA wire and composite wind turbine blade

Particulars	Value
Wind turbine blade-Glass fiber epoxy	
Young's modulus, E_C, GPa	4.5
Density, ρ_C, kg/m^3	950
Geometrical factors	
Bending moment of inertia, I, m^4	1.62e-6
Area of cross section at C_G, A, m^2	8.95e-4
SMA-Shape Memory Alloy (Nitinol)	
Young's modulus, GPa	
Martensite, E_M	15
Austenite, E_A	50
Density, ρ_S, kg/m^3	6450

6.25% shift in the first natural frequency and 30.23% reduction in displacement at 32Hz frequency. But at 30Hz the displacement is 4.59 mm which is 46.63% reduction in amplitude. Similarly, the smart blade excited at 2A, depicts a 73.16% reduction in amplitude at 25 Hz, the conventional blade's natural frequency.

6. Analytical validation of variation in dynamic parameters of smart blade

The variation in the natural frequency and the reduction in amplitude of vibration can be validated with help of an analytical model of cantilever composite beam. Influence of variation in SMA's properties at martensitic and austenite conditions, the wind turbine blade is considered to be a lumped mass system, with weight concentrating at center of gravity. The equation of a Euler beam is

$$\frac{d^2}{dx^2}\left(E_b I_b \frac{d^2 y(x)}{dx^2}\right) = \omega^2 \rho_b y(x) \tag{2}$$

where subscript b represents the beam's properties, ρ – Density (per unit length) and natural frequency of beam – ω. By considering the rules of mixture, the physical properties of beam can be written as

$$E_b = E_c + V_f(E_{MS} - E_c) \ \ and$$
$$\rho_b = \rho_c + V_f(\rho_S - \rho_c) \tag{3}$$

where V_f represents volume fraction of SMA embedded. EMS represents the young's modulus of SMA at martensitic phase and subscript c and s represent the physical properties of composite and shape memory alloy. The boundary conditions are provided for the conditions of cantilever beam as

$$\text{at } x = 0, y(x) = 0, \frac{dy(x)}{dx}=0,$$
$$\text{at } x=L, \ \frac{d^2y(x)}{dx^2}=0, \ \frac{d^3y(x)}{dx^3}=0 \tag{4}$$

applying the boundary conditions (3) and (4), the mathematical model providing the natural vibration of the cantilever beam is derived as

$$\omega^2 = \frac{\alpha_n^2[E_c + V_f(E_{MS} - E_c)]I}{l^4[\ \rho_c + V_f(\rho_S - \rho_c)]\mathrm{A}} \tag{5}$$

Where αn is the mode number corresponding to the flapwise vibration. The natural frequency of the composite beam is evaluated with a V_f=0.073% and with the physical and geometrical parameters of blade provided in Table 4.

The incorporation of relation between young's modulus of SMA across martensitic fraction, yields the influence of actuation current in natural frequency of blade. The Eq. (4) becomes

$$\omega^2(\xi) = \frac{\alpha_n^2[E_c + V_f(E_S(\xi) - E_c)]I}{l^4[\ \rho_c + V_f(\rho_S - \rho_c)]\mathrm{A}} \tag{6}$$

The model predicts the natural frequency of the blade to be 26.01 Hz, which is in acceptable range with the experimental result. The non-dimentionalised natural frequency of the blade is plotted across the actuation current and portrayed in Fig. 12.

The harmonic response of the blade can also be validated by formulating the magnification factor and incorporating the variation of young's modulus and damping factor across the actuation current. The magnification factor of the blade is expressed as

$$\mu = \frac{1}{\sqrt{(1 - r^2)^2 + (2\zeta(\xi)r)^2}} \tag{7}$$

where 'r' is the frequency ratio and ζ(ξ) is the damping factor variation with actuation current. The frequency ratio is obtained as the relation between the excitation frequency and natural frequency of the blade. The frequency ratio can be expressed as r=(ω_e/ω_n). Eq. (6) is substituted in the magnification factor, Eq. (7) becomes a function of volume fraction (V_f), Damping factor (ζ(ξ)) and actuation current.

The variation of natural frequency and magnification factor of the blade across the actuation current is portrayed in Fig. 13.

The reduction in the harmonic response of the blade, under actuated conditions validates the improvement in the damping of the structure. The shift in natural frequency of the beam is in relation with the volume fraction of SMA embedded on to the blade.

7. Comparison between analytical and experimental harmonic response of the smart blade

The modal analysis on the SMA embedded wind turbine blade under martensitic and austenite conditions of SMA, depicted the increase in natural frequency of blade with increase in actuation current. The similar increase is indicated in the analytical model. The increase in the natural across actuation current is due to the recovery stress increase the embedded SMA wires. This also increases the tensile stress in the composite beam, thus increasing the structural rigidity of the blade.

The volume fraction of SMA wires embedded should also be low as the compressive stress induced in the blade,

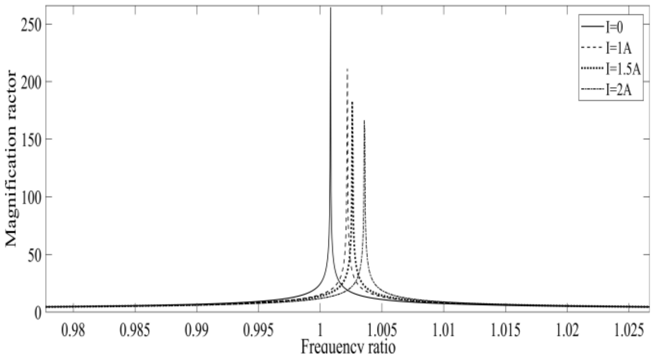

Fig. 13 Variation of Magnification factor across actuation current

Table 5 Reduction in vibration under actuation

Actuation current (A)	Magnification ctor at resonanc	Reduction in Mag. factor (%)	Amplitude of vibration at resonance (mm)	Reduction in amplitude of vibration(%)
0	264.5	~	8.6	~
1	211.2	20.15	6.61	23.14
1.5	183.2	30.74	6.26	27.21
2	166.5	37.05	6	30.23

due to actuation can cause compressive failure. The damping factor calculated for the variation is utilized in the analytical model of the smart blade in order to formulate the harmonic response of the blade.

Comparing reduction in the vibrational amplitude of the blade obtained through experimentation, to that of the numerical model, the percentage decrease in portrayed in Table 5.

The reduction depicted in the analytical model of the smart blade is within approval of the harmonic response of the smart blade under actuation. The harmonic response portrays the energy dissipation capability of SMA under martensitic and austenite conditions. The harmonic response also shows the reduction in amplitude of vibration under all excitation frequency and comparatively higher reduction at resonance.

8. Conclusions

The embedment of SMA wires on the conventional blade has shown improvement of damping, due to the super elastic nature of shape memory alloy. The increase in stiffness of the smart blade is also depicted by the 20% shift in the natural frequency of the blade. The 32.5% reduction in the amplitude of vibration at resonant condition, depicts the effectiveness of SMA at passive vibration control.

- Under actuation of SMA wires, the residual stress induced due to embedment results in the increase natural frequency of the smart blade.
- The heating of the smart blade, induced through actuation, causes the blade to become flexible thus increasing the structural damping of blade.
- The increase in damping can be inferred from the comparison of harmonic response of smart blade under different actuations.

- The analytical model of the smart blade under actuation current, depicted and validated the reduction in the harmonic response of the smart blade.
- Although the SMA embedment improves the structural integrity and dynamic characteristics of wind turbine blades, the volume fraction of SMA embedment is critical.
- The energy dissipation is higher with increase in the volume fraction of SMA, but the structure becomes more vulnerable to compressive stress under actuation.
- The analytical model, which simulates the actual response of the smart blade can be optimized for the volume fraction of SMA to be embedded, by provided the compressive stress induced as a constraint.

Acknowledgments

The authors would like to acknowledge Ministry of New and Renewable Energy (MNRE) India and PSG college of technology who have supported at various stages of this reported work.

References

Bhargaw, H.N., Ahmed, M. and Sinha, P. (2013), "Thermo-electric behaviour of niti shape memory alloy", *T. Nonferr. Metal Soc. China*, **23**(8), 2329-2335. https://doi.org/10.1016/S1003-6326(13)62737-5.

Zhao, Z., Chen, Z., Wang, X., HaoXu and Liu, H. (2016), "Wind-induced response of large-span structures based on pod-pseudo-excitation method", *Advan. Steel Constr*., **12**(1), 1-16.

Choi, S. and Lee, J.J. (1998), "The shape control of a composite beam with embedded shape memory alloy wire actuators", *Smart Mater. Struct*. **7**(6), 759-770.

Cromack, F.W. and Perkins D.E. (1978), "Wind turbine blade stress analysis and natural frequencies", Wind Energy Center Report.

Feng, W. and Gomez-Rivas, A. (2005), "An experimental approach for evaluating harmonic frequencies of a flexible beam", *Age*, **10**, 1-8.

Hu, Y. R. and Vukovich, G. (2005), "Active robust shape control of flexible structures", *Mechatronics*, **15**(7), 807-820. https://doi.org/10.1016/j.mechatronics.2005.02.004.

Irschik, H. (2002), "A review on static and dynamic shape control of structures by piezoelectric actuation", *Eng. Struct*., **24**(1), 5-11. https://doi.org/10.1016/S0141-0296(01)00081-5.

Kim, S. and Cho, M. (2010). "A simple smart wing actuator using ni-ti SMA", *J. Mech. Sci. Technol*., **24**(9), 1865-1873. https://doi.org/10.1007/s12206-010-0609-8.

Kumar, A., Dwivedi, A., Paliwal, V. and Patil, P.P. (2014), "Free vibration analysis of Al 2024 wind turbine blade designed for Uttarakhand region based on FEA", *Proc. Technol*., **14**, 336-347. https://doi.org/10.1016/j.protcy.2014.08.044.

Lau, K.T. (2002), "Control of natural frequencies of a clamped - clamped composite beam with embedded shape memory alloy wires", *Comp. Struct*., **58**(1), 39-47. https://doi.org/10.1016/S0263-8223(02)00042-9.

Lee, J.W., Han J.H., Shin, H.K. and Bang, H.J. (2014), "Active load control of wind turbine blade section with trailing edge flap: wind tunnel testing", *J. Intel. Mat. Syst. Str*., **25**(18), 2246-2255. https://doi.org/10.1177%2F1045389X14544143.

Lin, Y.J., Lee, T., Choi, B. and Saravanos, D. (1999), "An application of smart-structure technology to rotor blade tip vibration control", *J. Vib. Control*, **5**(4), 639-658. https://doi.org/10.1177%2F107754639900500408.

Martinez Vazquez, P. (2016), "Wind-induced vibrations of structures using design spectra", *Int. J. Advan. Struct. Eng*., **8**(4), 379-389. https://doi.org/10.1007/s40091-016-0139-4.

Mevada, H. and Patel, D. (2016), "Experimental Determination of Structural Damping of Different Materials", *Proc. Eng*., **144**, 110-115. http://10.1016/j.proeng.2016.05.013.

Mollasalehi, E., Sun, Q. and Wood, D. (2013), "Contribution of small wind turbine structural vibration to noise emission", *Energies*, **6**(8), 3669-3691. https://doi.org/10.3390/en6083669.

Mouleeswaran, S.K., Mani, Y., Keerthivasan, P. and Veeraragu, J. (2018), "Vibration control of small horizontal axis wind turbine blade with shape memory alloy", *Smart Struct. Syst*., **21**(3), 257-262. https://doi.org/10.12989/sss.2018.21.3.257.

Ni, Q.Q., Zhang, R.X., Natsuki, T. and Iwamoto, M. (2007), "Stiffness and vibration characteristics of SMA/ER3 composites with shape memory alloy short fibers", *Compos. Struct*., **79**(4), 501-507. https://doi.org/10.1016/j.compstruct.2006.02.009.

O'Toole, K.T., McGrath, M.M. and Coyle, E. (2009), "Analysis and evaluation of the dynamic performance of SMA actuators for prosthetic hand design", *J. Mat. Eng. Perform*., **18**(5-6), 781-786. https://doi.org/10.1007/s11665-009-9431-9.

Pabut, O., Allikas, G., Herranen, H., Talalaev, R. and Vene, K. (2012), "Model validation and structural analysis of a small wind turbine blade", 8th International DAAAAM Baltic Conference, Tallinn, Estonia, April.

Seelecke, S. and Muller, I. (2004), "Shape memory alloy actuators in smart structures: modeling and simulation", *Appl. Mech. Rev*. **57**(1), 23-46. https://doi.org/10.1115/1.1584064.

Sellami, T., Berriri, H., Darcherif, A.M., Jelassi, S. and Mimouni, M.F. (2016), "Modal and harmonic analysis of three-dimensional wind turbine models", *Wind Eng*., **40**(6), 518-527. https://doi.org/10.1177%2F0309524X16671093.

Simonović, A.M., Jovanović, M.M., Lukić, N.S., Zorić, N.D., Stupar, S.N. and Ilić, S.S. (2016), "Experimental studies on active vibration control of smart plate using a modified PID controller with optimal orientation of piezoelectric actuator", *J. Vib. Control*, **22**(11), 2619-2932. https://doi.org/10.1177%2F1077546314549037.

Song, G., Kelly, B. and Agrawal, B.N. (2000), "Active position control of a shape memory alloy wire actuated composite beam", *Smart Mater. Struct*. **9**(5), 711-716.

Umesh, K. and Ganguli, R. (2009), "Shape and vibration control of a smart composite plate with matrix cracks", *Smart Mater.. Struct*., **18**(2), 025002.

Vitiello, A., Giorleo, G. and Morace, R.E. (2005), "Analysis of thermomechanical behaviour of nitinol wires with high strain rates", *Smart Mater. Struct*. **14**(1), 215-221.

FR